

# 1 Stratigraphic templates for ice core records of the past 1.5 2 million years

3 Eric W. Wolff<sup>1</sup>, Hubertus Fischer<sup>2</sup>, Tas van Ommen<sup>3</sup>, David A. Hodell<sup>1</sup>

4 1. Dept of Earth Sciences, University of Cambridge, UK (ew428@cam.ac.uk)

5 2. Climate and Environmental Physics, Physics Institute & Oeschger Centre for Climate Change Research,  
6 University of Bern, Switzerland

7 3. Australian Antarctic Division and Australian Antarctic Program Partnership, University of Tasmania,  
8 Tasmania, Australia.

9 *Correspondence to:* Eric Wolff (ew428@cam.ac.uk)

10 **Abstract.** The international ice core community has a target to obtain continuous ice cores stretching back as far  
11 as 1.5 million years. This would provide vital data (including a CO<sub>2</sub> profile) allowing us to assess ideas about  
12 the cause of the Mid-Pleistocene Transition (MPT). The European Beyond EPICA project and the Australian  
13 Million Year Ice Core project each plan to drill such a core in the region known as Little Dome C. Dating the  
14 cores will be challenging, and one approach will be to match some of the records obtained with existing marine  
15 sediment datasets, informed by similarities in the existing 800 kyr period. Water isotopes in Antarctica have  
16 been shown to closely mirror deepwater temperature, estimated from Mg/Ca ratios of benthic foraminifera, in a  
17 marine core on the Chatham Rise near to New Zealand. The dust record in ice cores resembles very closely a  
18 South Atlantic marine record of iron accumulation rate. By assuming these relationships continue beyond 800  
19 ka, our ice core record could be synchronised to dated marine sediments. This could be supplemented, and allow  
20 synchronisation at higher resolution, by the identification of rapid millennial scale-events that are observed both  
21 in Antarctic methane records and in emerging records of planktic oxygen isotopes and alkenone sea surface  
22 temperature (SST) from the Portuguese Margin. Although published data remain quite sparse, it should also be  
23 possible to match <sup>10</sup>Be from ice cores to records of geomagnetic palaeointensity and authigenic <sup>10</sup>Be/<sup>9</sup>Be in  
24 marine sediments. However, there are a number of issues that have to be resolved before the ice core <sup>10</sup>Be record  
25 can be used. The approach of matching records to a template will be most successful if the new core is in  
26 stratigraphic order, but should also provide constraints on disordered records, if used in combination with  
27 absolute radiogenic ages.

28

## 29 1. Introduction

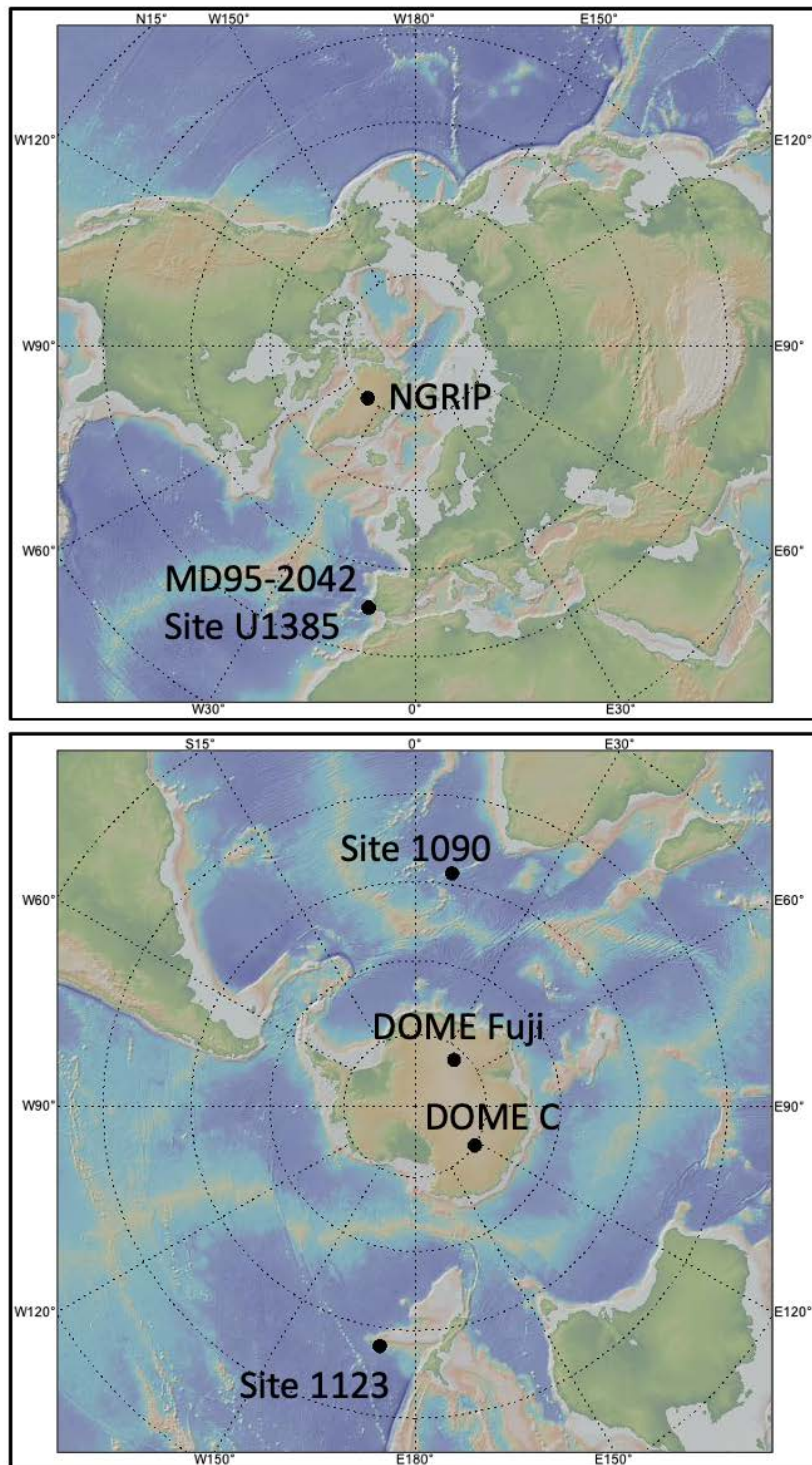
30 Ice cores have provided iconic records of changes in atmospheric composition and climate over  
31 glacial/interglacial cycles, with Antarctic datasets extending, so far, 800 kyr into the past (e.g. Bereiter et al.,  
32 2015; Jouzel et al., 2007; Wolff et al., 2010). While this illustrates what is often referred to as the “100 kyr  
33 world”, marine (e.g. Lisiecki and Raymo, 2005) and terrestrial records indicate that a different style and strength  
34 of glacial cycle existed earlier in the Pleistocene, during the “41 kyr world”. The change in amplitude and  
35 frequency is referred to as the mid-Pleistocene Transition (MPT) and occurs in the absence of any obvious  
36 change in astronomical forcing. The causes of the MPT remain hotly debated (Clark et al., 2006), with changes  
37 in CO<sub>2</sub> concentration or changes in the nature of the ice/rock interface underlying continental ice sheets often  
38 invoked.

39 Some of the issues surrounding these debates could be resolved if an ice core record, extending beyond the MPT  
40 and including records of past greenhouse gas concentrations, could be obtained. It has therefore become a key  
41 target of the ice core community to find a location to drill a core reaching as far back as 1.5 Ma (Fischer et al.,  
42 2013). Several projects to obtain such a core are partially underway, including the European Beyond EPICA  
43 project which plans to drill between 2021 and 2025 at a site known as Little Dome C (LDC). This site is only  
44 about 30 km from the site of the EPICA Dome C drilling (Fig. 1) that reached 800 ka, but is located on top of a  
45 subglacial highland, thus avoiding basal melting that led to loss of the oldest ice at Dome C. The Australian  
46 Million Year Ice Core (MYIC) project is targeting the same region of Antarctica.

47 A major challenge is to date such a core. Recently greenhouse gas concentrations were reported for ice as old as  
48 2 Ma at a blue ice location of Allan Hills, Antarctica (Yan et al., 2019). While this provided tantalising  
49 snapshots of atmospheric composition, the dating, using the <sup>40</sup>Ar atmospheric increase method (see below), was  
50 too imprecise (with a quoted uncertainty of 110 kyr or 10% of age) to assign data unequivocally to particular  
51 parts of glacial cycles, or even to specific cycles. While this is a particular issue for discontinuous records such  
52 as those from blue ice, dating is also likely to be a major problem for a “standard” core, even assuming it is  
53 complete and continuous.

54 A number of methods can be used to try and date the ice older than 800 ka. As with the blue ice, absolute ages  
55 may be estimated from radiometric methods, including <sup>81</sup>Kr decay (Buizert et al., 2014; Crotti et al., 2021), and  
56 the growth in atmospheric concentration with time of <sup>40</sup>Ar (Bender et al., 2008; Yan et al., 2019), but both of  
57 these methods currently have large error bars at ages of 1 million years or more. The decay of cosmogenic  
58 isotopes (using the ratio of <sup>10</sup>Be/<sup>36</sup>Cl to remove production rate variations) also has potential, but issues with  
59 <sup>36</sup>Cl loss at low accumulation rate sites (Delmas et al., 2004) have to be solved and the dating accuracy will  
60 likely be similar to the one using <sup>81</sup>Kr and <sup>40</sup>Ar.

61 While absolute methods can indicate the approximate age of the ice within the pre-MPT period, the uncertainty  
62 is currently too large to answer many of the questions that are relevant to such ice. For example, if changes in  
63 CO<sub>2</sub> did occur, it will be important to determine exactly when they occurred, and at what rate. Did the changes  
64 occur only in particular parts of each glacial cycle? In what part of glacial cycles did millennial events still occur  
65 before the MPT? All these questions require an age scale that is precise to within at worst a few millennia.



66

67 Figure 1. Location map. The maps show the locations of the ice and marine cores shown in this paper. Colours

68 represent topography and bathymetry. Figure made with GeoMapApp ([www.geomapapp.org](http://www.geomapapp.org)) / CC BY.

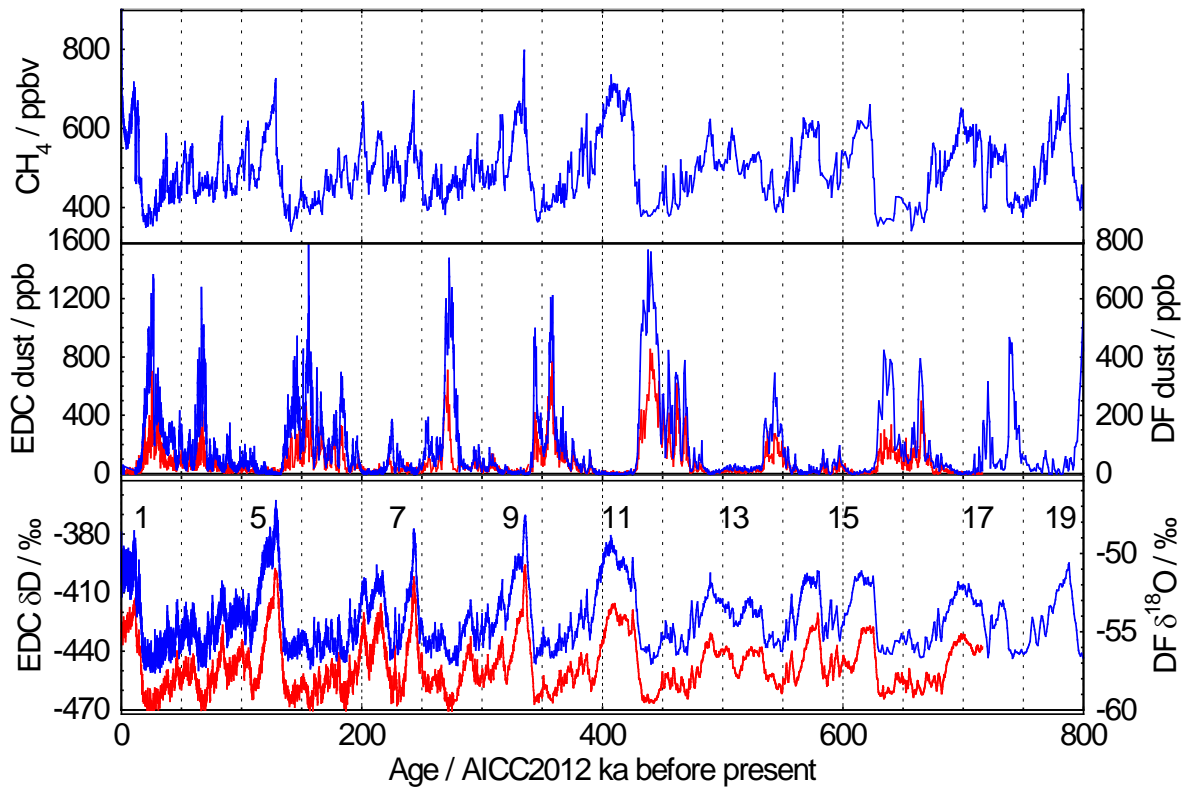
69 The main technique for dating the ice <800 ka in age has been to combine an estimate of past snow  
70 accumulation rate and thinning with a range of fixed points that tie the ice core to known ages (Bazin et al.,  
71 2013). These fixed points include the signal of low intensity of the geomagnetic dipole field associated with  
72 polarity reversals recorded as increases in  $^{10}\text{Be}$  deposition (Raisbeck et al., 2006), and various orbital tuning  
73 targets including  $\delta^{18}\text{O}_{\text{atm}}$  (Extier et al., 2018) and the ratio of  $\text{O}_2/\text{N}_2$  (Kawamura et al., 2007). These methods, as  
74 well as the radiometric ones, will certainly be applied to the new 1.5 Ma projects. However, diffusion, lack of  
75 resolution and disturbed ice flow, with the possibility of folded ice near the bed, as has been seen at deep ice  
76 core sites in Greenland (Grootes et al., 1993; NEEM Community Members, 2013), mean that further  
77 stratigraphic methods to date the core may be needed.

78 One additional option is to create templates to which the records generated in the new projects can be matched.  
79 The orbital targets (for tuning of  $\text{O}_2/\text{N}_2$  and  $\delta^{18}\text{O}_{\text{atm}}$ ) used to construct the 800 ka age model (Bazin et al., 2013)  
80 are simple examples of the use of such templates, and will not be included here as they are very straightforward  
81 to construct. Marine and terrestrial records that are rather well-dated extend beyond 1.5 million years. As an  
82 example many marine records have been mapped, using benthic isotopes, onto the LR04 marine stack (Lisiecki  
83 and Raymo, 2007), whose age uncertainty at 1.5 Ma is estimated at 6 kyr, or the more recent Prob-Stack (Ahn et  
84 al., 2017), which also uses the LR04 age model. Alignments such as these would allow age uncertainties of the  
85 order needed to answer the questions about timing of  $\text{CO}_2$  and millennial change discussed above. The  
86 drawback is that they obviously preclude the option of assessing phasing between ice records and the (marine)  
87 templates, as such a phase has to be assumed. In the absence of better dating methods, this cannot be avoided.

88 In this paper, we consider which ice core parameters may have analogues in the marine record that could be  
89 used as templates onto which a future ice core could be mapped. We focus particularly on the EPICA Dome C  
90 ice core (EDC), because its close proximity to the planned ice cores at LDC leads us to expect a similar signal in  
91 most parameters. We use ice core datasets which have already been shown to closely mirror a particular marine  
92 record over the past 800 kyr. We consider the mechanistic basis for such agreement and whether it is likely to  
93 apply through the MPT to 1.5 Ma. We then present “predictions” of what some parameters might look like in  
94 the new ice core, which can be used as both a test of integrity and continuity, and as a first dating tool for the  
95 core.

## 96 **2. EPICA Dome C ice core records**

97 In the following sections, we will consider possible analogues for 4 ice core parameters (Fig. 2). The water  
98 isotope record ( $\delta^{18}\text{O}$  and  $\delta\text{D}$ ) is the most basic climate parameter (Jouzel et al., 2007) recorded in the ice,  
99 generally considered to represent temperature at the ice core site. Dust is the insoluble component of impurities  
100 trapped in the ice, and represents terrestrial material from the southern continents. Both dust and water isotopes  
101 display particularly strong changes over glacial cycles with more subdued millennial scale variations. Methane  
102 is the one component in the ice core record that displays abrupt events, parallel to the rapid Dansgaard-Oeschger  
103 events seen in Greenland ice cores.  $^{10}\text{Be}$  (not shown in Fig. 2) is the cosmogenic isotope most commonly  
104 measured in ice, and its production is controlled by changes in Earth’s and the Sun’s magnetic fields which also  
105 influence cosmogenic isotopes archived in other material. These 4 components will be considered in more  
106 detail in the following sections.



107  
 108 Figure 2. Ice core data over the past 800 kyr. Ice core records covering the past 800 kyr from Dome C (blue) and  
 109 from the last 720 kyr from Dome Fuji (red). Top panel: methane (Louergue et al., 2008); middle panel: dust  
 110 (Kawamura et al., 2017; Lambert et al., 2008); lower panel: water isotopes (Jouzel et al., 2007; Kawamura et al.,  
 111 2017), with interglacial marine isotope stage numbers marked.

112  
 113 Although we are specifically aiming here to create a template for the European or Australian drilling at LDC, we  
 114 note that in most details, the features and relative changes seen for water isotopes, dust and <sup>10</sup>Be are expected to  
 115 be similar across the East Antarctic plateau. This is illustrated in Fig. 2, where we have plotted  $\delta^{18}\text{O}$  and dust  
 116 concentration from Dome Fuji (Fig. 1) (Kawamura et al., 2017) along with  $\delta\text{D}$  (Jouzel et al., 2007) and dust  
 117 concentration (Lambert et al., 2008) from EDC, all plotted on the AICC2012 age scale. The absolute level of  
 118 dust concentrations varies spatially across the Antarctic plateau, being dependent on travel distance from the  
 119 main Patagonian dust source region (Fischer et al., 2007a) and concentrations are higher at Dome Fuji than at  
 120 Dome C. This difference is explained in part because of the different analysis method used for Dome F and  
 121 Dome C that includes different size ranges, but in any case the pattern is almost identical on multimillennial  
 122 timescales; methane is of course expected to show the same concentrations across Antarctica. Our templates for  
 123 LDC are therefore likely to serve as equally valid for other sites across East Antarctica.

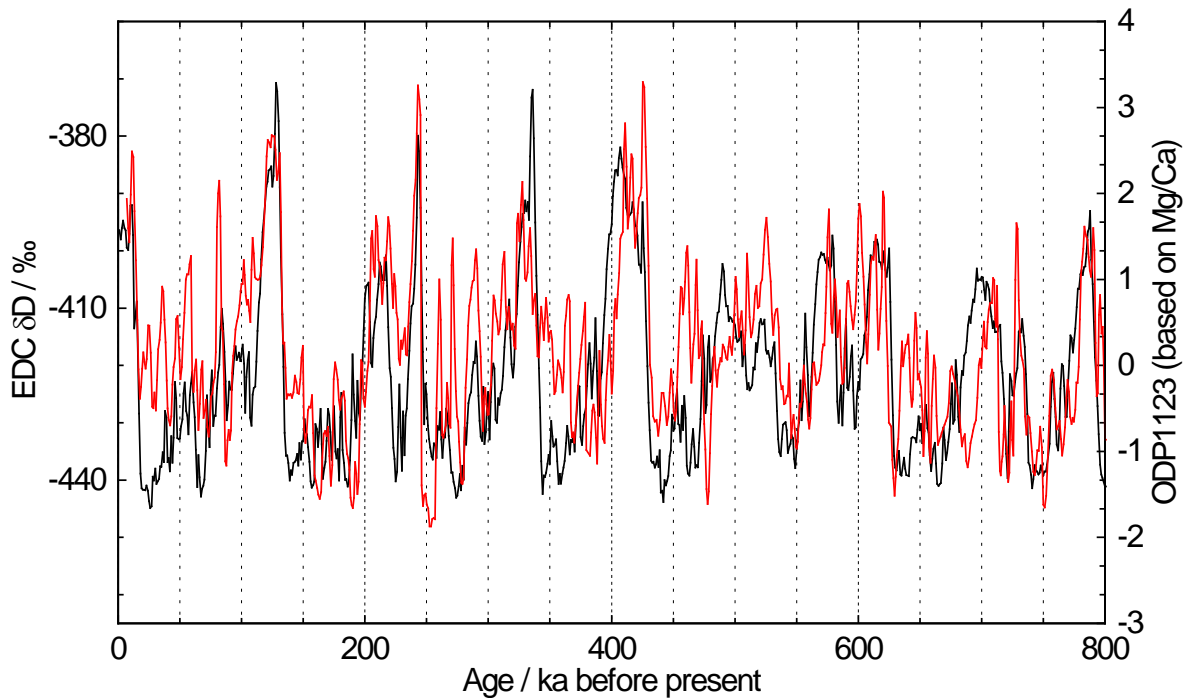
124 **3. Water isotopes**

125 Water isotopes ( $\delta\text{D}$ ,  $\delta^{18}\text{O}$ ) in ice cores are generally taken to represent the temperature at the ice core site,  
 126 although the reality is actually much more complicated than that (Buizert et al., 2021; Jouzel et al., 1997). It  
 127 therefore makes sense to look for a potential marine analogue that also records mainly temperature. Although  
 128 water isotope records from ice are sometimes plotted along with oxygen isotope records from marine cores, the

129 latter reflect a combination of temperature and ice volume (as well as local salinity effects), and so the  
130 variability of the two records may not be comparable on glacial-interglacial scales. A commonly used  
131 geochemical temperature sensor in marine cores is the ratio of Mg/Ca in foraminifera.

132 Planktic Mg/Ca records, covering 800 ka and more, are available from a number of marine sites and should  
133 reflect sea surface temperatures (SSTs) (e.g. Shakun et al., 2015). However while we expect some match  
134 between Antarctic temperatures and those from the high southern latitudes, we would expect most other sites to  
135 display a rather different pattern owing to the operation of the bipolar seesaw (e.g. Barker et al., 2011).  
136 Elderfield et al. (2012) noticed a striking similarity between the deepwater temperature inferred from Mg/Ca of  
137 benthic foraminifera at Ocean Drilling Program (ODP) site 1123 (Fig. 1), on the Chatham Rise east of New  
138 Zealand, and the temperature inferred from  $\delta D$  in the EDC ice core. They hypothesised that this is because  
139 deepwater temperature, particularly in the South Pacific, reflects the temperature of sinking surface waters and  
140 of Antarctic and proximal air temperature. Mean ocean temperature (determined by analysing noble gas ratios  
141 in ice cores) also shows a very similar pattern to Antarctic surface temperature across the last two glacial  
142 terminations (Baggenstos et al., 2019; Bereiter et al., 2018; Shackleton et al., 2020; Shackleton et al., 2021),  
143 which supports the interpretation. In recent years, deep water temperatures covering at least 1.5 Ma have been  
144 obtained from two other sites in the North Atlantic (Sosdian and Rosenthal, 2009) and North Pacific (Ford and  
145 Raymo, 2019), but given their location they are not expected to reflect Antarctic climate so directly, thus leaving  
146 only ODP site 1123 as a suitable comparator.

147 In Figure 3, we compare the record of  $\delta D$  from EDC with that of benthic Mg/Ca from site 1123 over the last 800  
148 ka. The Mg/Ca record is presented as converted to temperature and interpolated (Elderfield et al., 2012), and is  
149 on the LR04 age model (Lisiecki and Raymo, 2005), while the ice core data is on AICC2012 (Bazin et al.,  
150 2013). By using a suitable amplitude scaling to overlay the two records we can compare their fidelity to each  
151 other and observe the extended Mg/Ca record as a possible template for  $\delta D$  over 1.5 Ma.



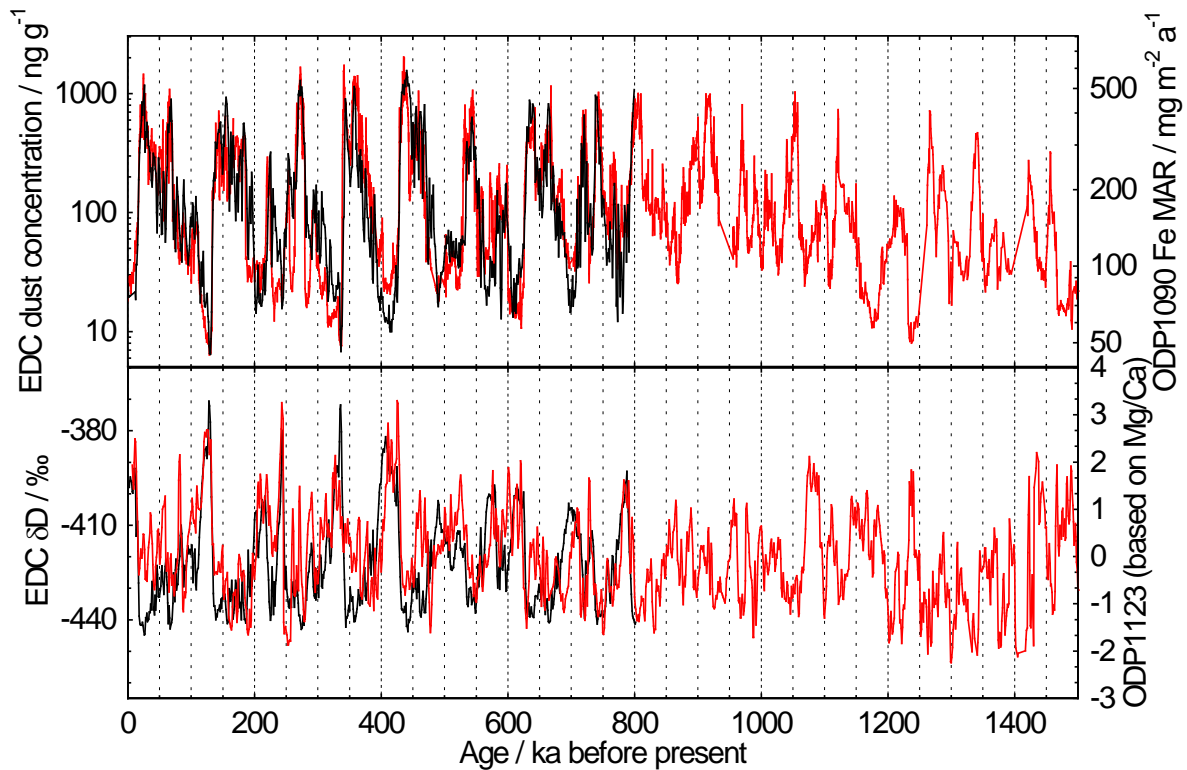
152  
 153 Figure 3. Ice core and marine sediment data reflecting temperature for the past 800 kyr. EDC deuterium (black,  
 154 AICC2012 age scale) (Jouzel et al., 2007). ODP site 1123 deepwater temperature (red, LR04 age model), based  
 155 on Mg/Ca (Elderfield et al., 2012).

156  
 157 The similarity between the two records is strong at the orbital timescale where both the shape and the relative  
 158 amplitude of each glacial cycle is the same in the two records. The correlation coefficient between the two  
 159 records after they are aligned in time is 0.67 (Elderfield et al., 2012) ( $r^2 = 0.45$ ). However, there are significant  
 160 mismatches at the shorter, multimillennial, timescale. Some very prominent millennial-scale AIM (Antarctic  
 161 isotopic Maximum) events in the ice core record are very weak, or in some cases not clearly resolved, in the  
 162 marine record. Some of the issues may actually be related to temporal synchronisation, and perhaps to the  
 163 resolution of the marine record. But still, it would be hard to use the marine record as a template for an ice core  
 164 record between 450 and 550 ka (MIS 13). This is a concern because some of the sections of Site 1123 beyond  
 165 800 ka have a similar nature (in terms of signal amplitude) to that section.

166 Despite these concerns over the fidelity of the marine record as a predictor of the ice core isotope signal, we  
 167 would expect the similarity to continue provided deepwater temperature at high southern latitudes continues to  
 168 be driven by surface temperatures around Antarctica before the MPT. What could disrupt such a link would be  
 169 significant changes in ocean circulation and in the reach of different water masses. Such changes may well have  
 170 occurred over the MPT (Ford and Raymo, 2019), and one suggestion is that they are related to a hypothesised  
 171 change in the Antarctic Ice Sheet (Raymo et al., 2006) from largely terrestrial to marine-based. While such  
 172 changes would certainly have impacted the supply of water affected by Antarctic surface temperatures to the  
 173 deep ocean, the proximity of site 1123 to Antarctica makes it unlikely that a southern influence was completely  
 174 absent at that time. We therefore see it as likely that the site 1123 Mg/Ca record extended to 1.5 Ma (Fig. 4)  
 175 does serve as an approximate template for at least the glacial/interglacial variability in Antarctic temperature and



176 therefore LDC deuterium. However, we accept the possibility that the exact nature of the relationship between  
177 the two records could have differed in the early part of the period from that observed after 800 ka, and indeed  
178 should a mismatch be found in the ice core record it will provoke reconsideration of the assumptions made here.



179  
180 Figure 4. Ice core records to 800 ka and marine records to 1500 ka. Lower panel: EDC deuterium  
181 (Jouzel et al., 2007) and Mg/Ca-based deepwater temperature (red) from site ODP1123 (Elderfield et al., 2012).  
182 Upper panel: EDC dust (black) (Lambert et al., 2008) and Fe MAR from ODP site 1090 (Martinez-Garcia  
183 et al., 2011).

184  
185 It would obviously be beneficial to search for other marine analogues of Antarctic temperature. The similarity of  
186 benthic oxygen isotopes in cores on the Portuguese Margin to Antarctic temperature was noted previously,  
187 albeit on a very short time period (Shackleton et al., 2000). The extension of this record, which is underway  
188 (Birner et al., 2016) would provide a much better resolved record, with clear millennial scale signals, and its  
189 applicability as a template could be assessed. The caveat is that the underpinning reason for similarity of a  
190 benthic isotope record controlled by several factors (ice volume, temperature, hydrography and water mass  
191 changes) with Antarctic temperature at such a distal site is unclear, making it difficult to assess the likelihood  
192 that the relationship persisted before the MPT.

#### 193 4. Dust

194 Terrestrial dust is measured directly in ice cores, as insoluble particle numbers and sizes which can be converted  
195 to mass concentrations, and indirectly in marine sediments through the concentrations or ratios of elements that  
196 are mainly (at appropriate sites) of windborne terrestrial origin. The 800 ka record of dust concentration in the

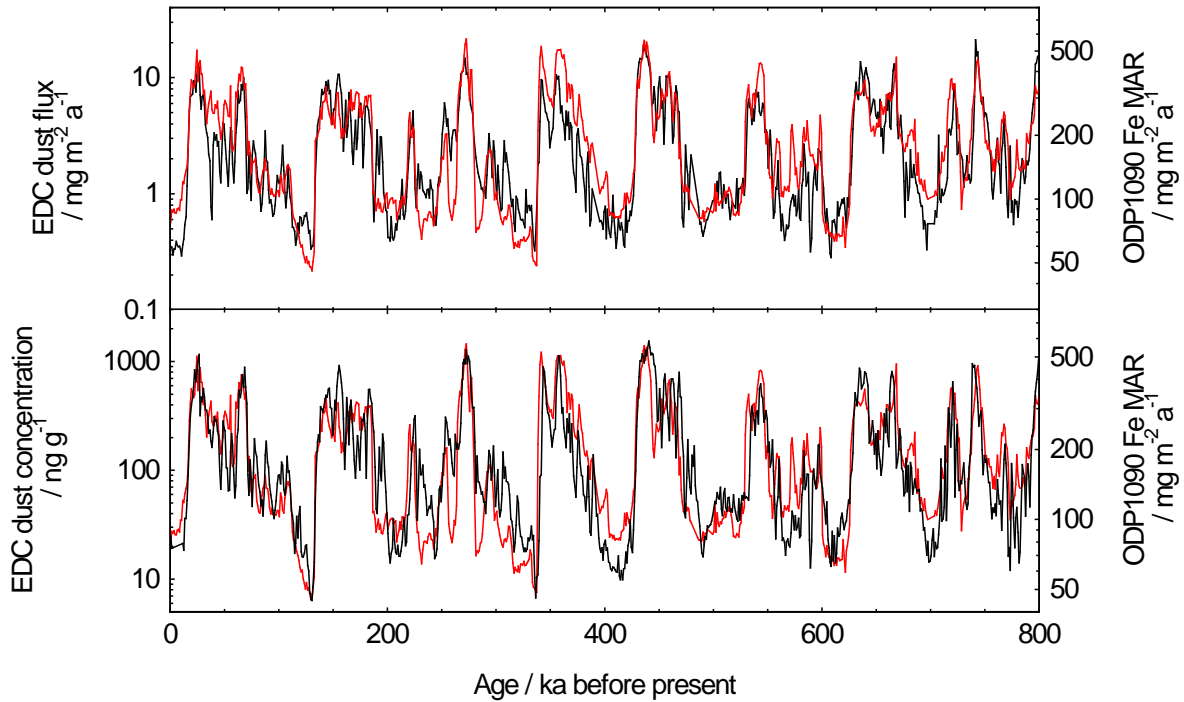


197 EDC ice core (Lambert et al., 2008) shows strong glacial-interglacial cycles, with high concentrations of dust in  
198 glacial periods, and some multimillennial scale variability. Elemental and isotopic analysis indicates that the  
199 dust mainly originates from South American sources, particularly in Patagonia (Delmonte et al., 2008). As a  
200 result we would expect a close relationship between dust arriving in Antarctica and dust deposited onto the  
201 South Atlantic during the early stages of the path to Antarctica.

202 ODP site 1090 (Fig. 1) is ideally located to sample dust during its transport in the westerly wind belt from the  
203 Patagonian sources towards Antarctica. Martinez-Garcia et al. (2011) noted that different dust proxies in the  
204 sediment core from site 1090 matched well with each other over 4 Ma, and with EDC dust flux over 800 ka.  
205 Here we compare their preferred dust proxy (mass accumulation rate of iron, Fe MAR) with the dust  
206 concentration at EDC (Lambert et al., 2008). We prefer to use concentration rather than flux because this is what  
207 we will be able to measure in the deeper parts of the LDC core – the flux is a derived quantity that requires  
208 knowledge of the snow accumulation rate. It is therefore a fairer test to assess the similarity of the measured  
209 quantity (concentration) to the marine target. In the section of the paper on <sup>10</sup>Be, we do discuss the potential to  
210 use water isotopes to derive snow accumulation rate and hence calculate fluxes. This could also be done for  
211 dust, if it were considered essential, but it carries some risk because of the assumptions involved.

212 In Fig. 5 we compare the two records over the last 800 ka, showing the result both for EDC dust concentration  
213 and for flux. Note that glacialials have high values of dust, that both records have been smoothed to 1 ka averages,  
214 and are plotted on log scales. With the appropriate amplitude scaling, the agreement between the two records is  
215 remarkable. This applies both to the consistent amplitude relationship, to the shape of glacial-interglacial  
216 cycles, and to the identification of almost every multimillennial scale peak in both records. The section from  
217 450-550 ka, which was problematical in the isotope records discussed above, shows a good match. The  
218 correlation coefficient between EDC dust and ODP1090 Fe Mar is 0.83 ( $r^2=0.69$ ) both for EDC dust  
219 concentration and flux.

220



221  
 222 Figure 5. Ice core and marine sediment dust data for the past 800 kyr. EDC dust (black) (Lambert et al., 2008);  
 223 Fe MAR from ODP site 1090 (red) (Martinez-Garcia et al., 2011). Top panel uses EDC dust flux, while lower  
 224 panel uses EDC dust concentration. Data have been smoothed to 1 kyr averages and the marine data were  
 225 aligned (Martinez-Garcia et al., 2011) to the ice core age model.

226  
 227 The agreement is made more surprising by the fact that the dynamic range of the two records is very different:  
 228 the marine dust, being geographically closer to the dust production in Patagonia than is the long-range  
 229 transported ice core record, varies by a factor 10 (minimum in MIS 5e, maximum in MIS 13), while the ice core  
 230 dust concentration varies by a factor >100 (factor 200 between MIS 5e and MIS 13). The range of dust flux at  
 231 EDC would be about a factor 50, because the snow accumulation rate is about four times higher in MIS 5e than  
 232 in MIS 13. This implies that the causes of dust variability are split into two halves: a factor of about 10 is due  
 233 mainly to changes at or near the source of the dust, another factor of about 5 is due to changes in lifetime during  
 234 the long meridional journey to Antarctica. This has been discussed several times before (Fischer et al., 2007b;  
 235 Lambert et al., 2008; Markle et al., 2018; Petit and Delmonte, 2009; Wolff et al., 2010) and although the  
 236 different approaches led to somewhat different amplification factors by dust source and transport processes, the  
 237 comparison shows that solutions that match the available data must consider changes both in source and in  
 238 lifetime. We note that it is the very high dynamic range of the dust concentration or flux record in ice that  
 239 makes it possible to use raw concentrations in our comparisons – the relatively small factor change in  
 240 accumulation rate is overwhelmed by the factor 50 flux change, so that the same features seen in marine and ice  
 241 dust flux are still seen in ice concentration.

242 This implies that the extended marine dust record (Fig. 4) could be an excellent template for the dust record  
 243 expected in the LDC ice cores. The part of the variance that is based on changes at or near the source should  
 244 remain, whatever occurred across the MPT. The second part of the variability, arising from changes in aerosol

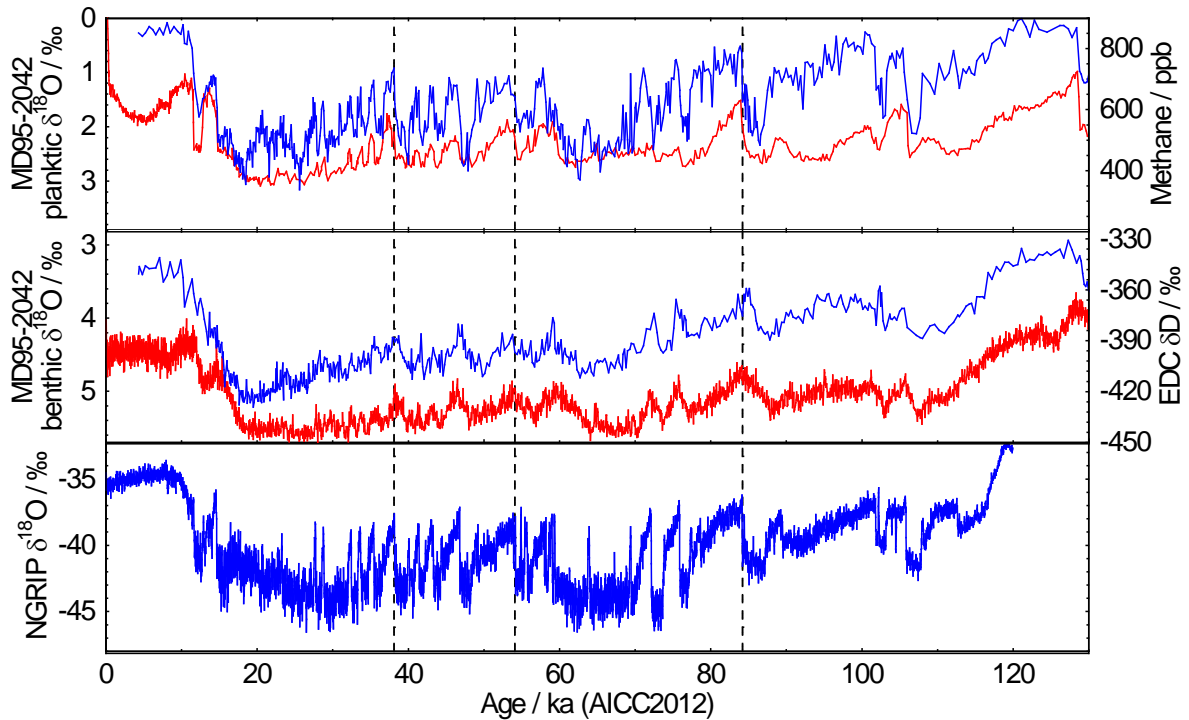
245 lifetime over the Southern Ocean, has been in phase with changes at the source over the last 800 ka. This could  
246 in theory have altered if there were major changes in atmospheric circulation across the MPT. Nonetheless, the  
247 major part of the variability (that arising from changes at the source and at the start of the transport route) will  
248 have remained unchanged. This implies that the basic glacial-interglacial pattern, as well as the imprint of  
249 millennial scale change will have persisted. The one circumstance in which this would not be the case is that in  
250 which a substantial new, local source of dust from the Antarctic margins existed. It has been suggested that one  
251 aspect of the MPT might have been a change in the Antarctic ice sheet, with more terrestrial (rather than marine)  
252 margins before the MPT (Raymo et al., 2006). Before using the dust record in the way we have proposed, it will  
253 be important to check for the presence of new dust sources, through for example isotopic analysis of dust to  
254 fingerprint its source area (Delmonte et al., 2008).

## 255 **5. Methane as a pattern for Dansgaard-Oeschger variability**

256 While the EDC water isotope and dust records show strong variability, particularly on orbital timescales, that  
257 can be used for pattern matching, their variations tend to be smooth, so that correlation is clear but imprecise.  
258 Records containing the imprint of Dansgaard-Oeschger (D-O) events have the capacity to identify sharp time  
259 points, and therefore to give much closer synchronisation, and many more clear tie points. Using the model of  
260 the bipolar seesaw, it is possible to rather convincingly reproduce D-O events from the Antarctic isotope record,  
261 to produce what is known as the synthetic Greenland record ( $GL_T$ -syn) (Barker et al., 2011). However, the  
262 synthetic record can never have the sharpness of the original signal and in particular for ice older than 800 kyr  
263 diffusion in the ice may have smoothed the higher frequency climate signal in the water isotope record. The only  
264 record in Antarctic ice that does retain the character of the D-O events is the methane record.

265 Over the last glacial cycle, every significant D-O event recorded in the Greenland ice core record (North  
266 Greenland Ice-Core Project (NorthGRIP) Members, 2004) is also seen in the EDC methane record (Loulergue et  
267 al., 2008) (Fig. 6). The same pattern of abrupt climate change is seen in many other northern hemisphere  
268 climate records, with a particularly faithful representation observed in planktonic oxygen isotope and alkenone  
269 SST data from marine sediment cores from the Portuguese Margin (Govin et al., 2014; Shackleton et al., 2000).  
270 Note that the benthic  $\delta^{18}O$  from the Portuguese Margin strongly resembles the water isotope record from  
271 Antarctica (here,  $\delta D$  from EDC) and that the phasing of planktic and benthic  $\delta^{18}O$  on the Iberian Margin is the  
272 same as that seen between  $CH_4$  and  $\delta D$  in the Antarctic ice core record. This pattern has been interpreted as  
273 being indicative of a thermal bipolar seesaw, and offers another signature for matching ice core and marine  
274 records.

275 While the planktonic oxygen isotope and alkenone SST records reproduce the NGRIP (Greenland) ice core  
276 isotopic record well in terms both of shape and amplitude, the methane record is less easy to match to the marine  
277 record. This is because the amplitude of methane change in comparison to isotopic change (in either the  
278 Greenland ice or North Atlantic marine record) is very variable. For example Greenland Interstadial (GI) 19 (at  
279 73 ka) is very strong in the isotope records but shows a methane amplitude of only 70 ppb (Baumgartner et al.,  
280 2014), and a sensitivity (methane jump/Greenland temperature change) less than a third of some other events.  
281 This means that, in an unknown section of older core, we could only expect to make unequivocal matches for  
282 some D-O events.

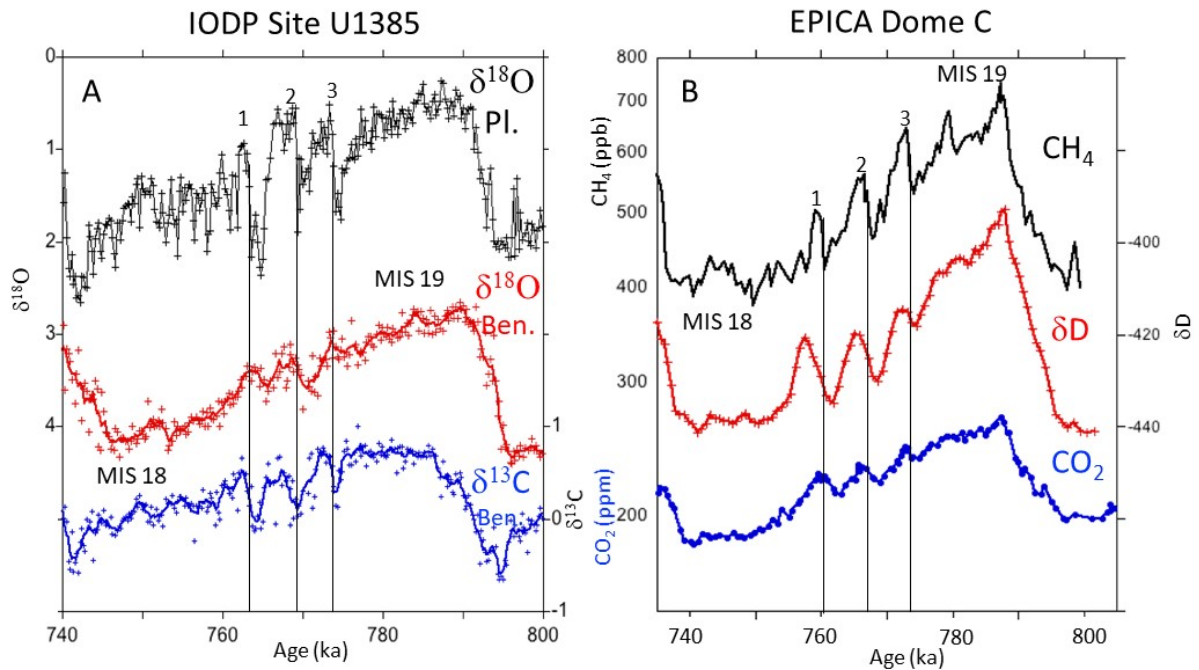


283  
 284 Figure 6. Sharp millennial scale features in the last glacial cycle. Bottom panel: NGRIP  $\delta^{18}\text{O}$  showing the  
 285 pattern of Dansgaard-Oeschger events (North Greenland Ice Core Project Members, 2004). Middle panel:  
 286 Benthic  $\delta^{18}\text{O}$  (blue) from site MD95-2042 (Govin et al., 2014; Shackleton et al., 2000) and the deuterium  
 287 record from the Antarctic EDC ice core (Jouzel et al., 2007). Upper panel: Planktonic  $\delta^{18}\text{O}$  (blue) from site  
 288 MD95-2042 (Govin et al., 2014; Shackleton et al., 2000) showing the same pattern as Greenland  $\delta^{18}\text{O}$ ; methane  
 289 from the Antarctic EDC ice core (red) (Louergue et al., 2008) showing a more subdued version of the same  
 290 variability. Vertical lines mark examples of the sharp onsets of three interglacials (Greenland Interstadial (GI) 8,  
 291 14 and 21).

292  
 293 High resolution isotopic data and alkenone SST collected at site U1385 (Fig. 1), extending to 1.45 Ma (Hodell et  
 294 al., 2015), located close (25 km) to core MD95-2042 (discussed above and shown in Fig. 6) indicate that events  
 295 of a D-O nature extend throughout the past 1.45 Myr (Birner et al., 2016). Thus the planktonic isotope and SST  
 296 records from that site, soon to be published, should serve as a regional template for D-O variability. Using it  
 297 with the methane ice core record makes the assumption that the teleconnection between North Atlantic climate  
 298 variability and the (predominantly tropical) methane sources (Bock et al., 2017) remained intact before the  
 299 MPT. This could be tested if East Asian speleothem records extended deeper in time than is currently the case  
 300 (Cheng et al., 2016).

301 As an example of the potential for this method, we examine the relationship between the oldest part of the EDC  
 302 record (MIS 19) and the equivalent data from site U1385 (Fig. 7). Here we can clearly identify the three strong  
 303 millennial events on the MIS 19/18 boundary in both the marine and ice core record, with the sharp onsets in  
 304 planktonic  $\delta^{18}\text{O}$  (marine) and methane (ice) and the more symmetric change in benthic  $\delta^{18}\text{O}$  (marine) and  $\delta\text{D}$   
 305 (ice). Carbon cycle data in both records also show the signature of the events. Radiometric ages are also

306 available in records that show these millennial events, adding further value to the correlations (Giaccio et al.,  
 307 2015). We note that one event (at about 780 ka) in the ice core record is not observed in the marine record,  
 308 despite the record having adequate resolution for its appearance.



309  
 310 Figure 7. (A) Planktonic  $\delta^{18}\text{O}$  (black), benthic  $\delta^{18}\text{O}$  (red) and  $\delta^{13}\text{C}$  (blue) over the MIS19-18 transition at Site  
 311 U1385 (Sánchez Goñi et al., 2016) compared to (B)  $\text{CH}_4$  (black),  $\delta\text{D}$  (red) and atmospheric  $\text{CO}_2$  (blue) in the  
 312 EPICA Dome C ice core. Three strong millennial events (labeled 1-3) occur on the MIS19-18 transition that are  
 313 recorded in both the marine sediment and ice cores. Vertical dashed lines are drawn at the abrupt transitions  
 314 from cold stadials to warmer interstadial conditions. Note that the phasing of ice core  $\text{CH}_4$  and  $\delta\text{D}$  is not quite as  
 315 expected from later time periods (Fig. 6) and may reflect uncertainty in  $\Delta$ -age (the age difference between the  
 316 ice and gas records).

317  
 318 The variable amplitude of methane peaks relative to North Atlantic records may make it harder to use than some  
 319 other records. Nonetheless the simplicity of the match at  $\sim 770$  ka suggests that methane in ice for the most  
 320 prominent millennial-scale features, used in a complementary way with other records, and matched against the  
 321 Portuguese Margin datasets, will provide a viable way of aligning the marine and ice records rather precisely at  
 322 least for the cycles immediately below 800 ka. In the highly thinned ice over 1.2 Ma old, where there may be  
 323  $>10$  ka/m of ice (Lilien et al., 2021), the use of high-resolution continuous online laser spectrometric  
 324 measurement techniques to measure  $\text{CH}_4$  (Chappellaz et al., 2013; Rhodes et al., 2015) should still allow  
 325 resolution of millennial features provided diffusion of methane (Bereiter et al., 2014) and of  $\delta\text{D}$  (Pol et al.,  
 326 2010) is limited.

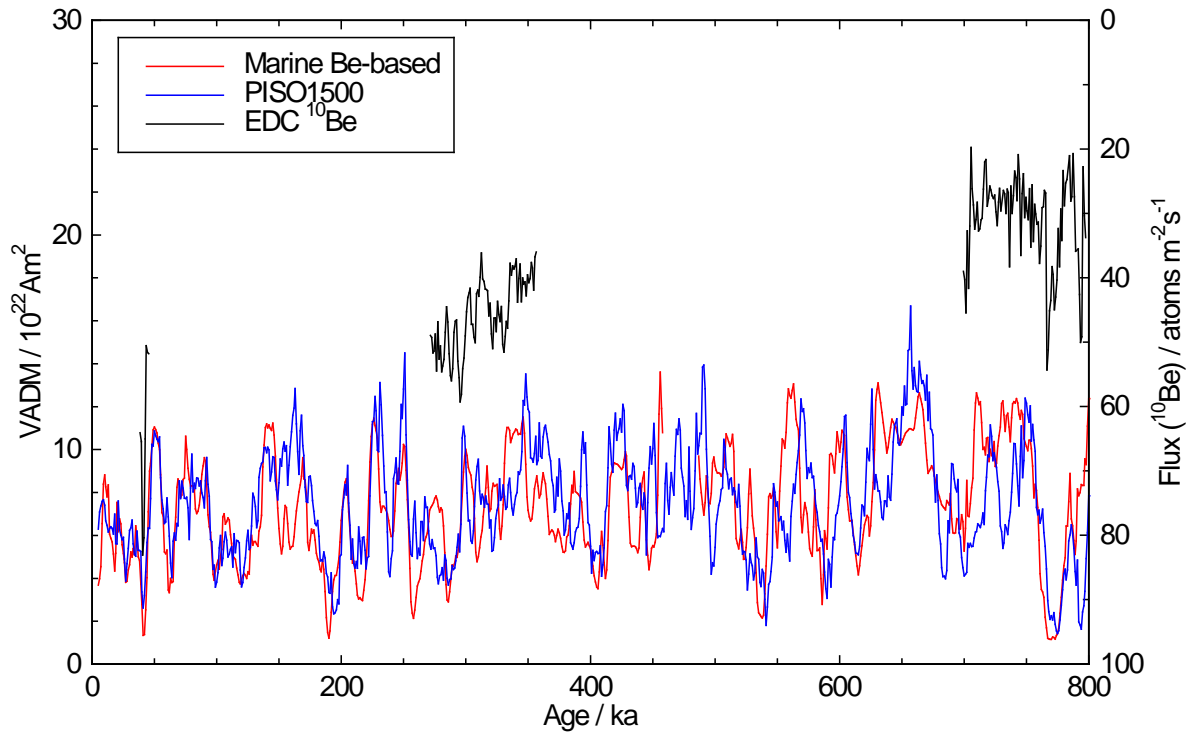
327 **6. <sup>10</sup>Be**

328 The production of <sup>10</sup>Be in the atmosphere, and its subsequent deposition to Antarctic snow, is controlled by the  
329 flux of cosmic rays, which in turn is influenced by the solar magnetic field (showing solar cycles), and on longer  
330 timescales by changes in intensity of Earth's magnetic field. As examples, centennial scale variations in <sup>10</sup>Be in  
331 ice over the last 14 kyr can be matched to variations in <sup>14</sup>C (Muscheler et al., 2014), while the Laschamp  
332 magnetic excursion at about 41 kyr BP (Raisbeck et al., 2017) and the Brunhes-Matuyama magnetic reversal at  
333 about 780 kyr BP (Raisbeck et al., 2006) are easily identified in ice cores. However there are, as with all  
334 aerosol-bound proxies, atmospheric transport influences on the relative amount of produced <sup>10</sup>Be that is  
335 transported to Antarctica. Additionally, in the central East Antarctic plateau the concentration of <sup>10</sup>Be shows a  
336 very clear imprint of climate that is mainly removed by calculating the flux. We will therefore have to  
337 independently estimate the snow accumulation rate in order to use any <sup>10</sup>Be template for dating.

338 In the marine record, the strength of Earth's magnetic field is imprinted in records of geomagnetic  
339 palaeointensity. A number of reconstructions have been made using individual cores, but a carefully constructed  
340 stack from different sites is especially valuable. The PISO-1500 stack of relative palaeointensity (RPI)  
341 (Channell et al., 2009) is particularly widely used, and could serve as a template for long-term variations in ice  
342 core <sup>10</sup>Be. In theory an even more direct comparator would be an index derived from the authigenic <sup>10</sup>Be/<sup>9</sup>Be  
343 ratios in marine sediments (Simon et al., 2018; Simon et al., 2016). Measurements extend beyond 2 Ma, and  
344 show a good correlation with the RPI (Channell et al., 2009). However because detailed <sup>10</sup>Be data exist only for  
345 a very few cores, the RPI might be considered a more robust dataset at this stage.

346 Both RPI and <sup>10</sup>Be/<sup>9</sup>Be show the strong features that we know have been seen in the ice core record: in  
347 particular the Laschamp excursion and the Brunhes-Matuyama boundary. It has been reported that the PISO-  
348 1500 stack shows a good correlation with the unpublished record of <sup>10</sup>Be flux from 200-800 ka (Cauquoin,  
349 2013), with a correlation coefficient reported as r=0.62 after the timescales have been aligned. Unfortunately,  
350 we can only show the comparison for the few published sections of ice (Fig 8).

351 The extended datasets, both of palaeointensity (Channell et al., 2009) and authigenic <sup>10</sup>Be/<sup>9</sup>Be ratios (Simon et  
352 al., 2018) should therefore be useful templates with which to compare the <sup>10</sup>Be data obtained from the LDC ice  
353 core. In Fig. 9 we show these two datasets, as an indication of what a <sup>10</sup>Be flux record from the new core should  
354 show. Note that uncorrected <sup>10</sup>Be/<sup>9</sup>Be data automatically include the degree of decay (1.39 Myr half-life) that  
355 will also apply in the ice core, whereas the PISO1500 do not include that decay. The paleointensity lows  
356 associated with polarity reversals in particular (Fig. 9) should be quite prominent in the <sup>10</sup>Be record (analogous  
357 to the Brunhes/Matuyama boundary). Some of the other prominent excursions events should also be captured.



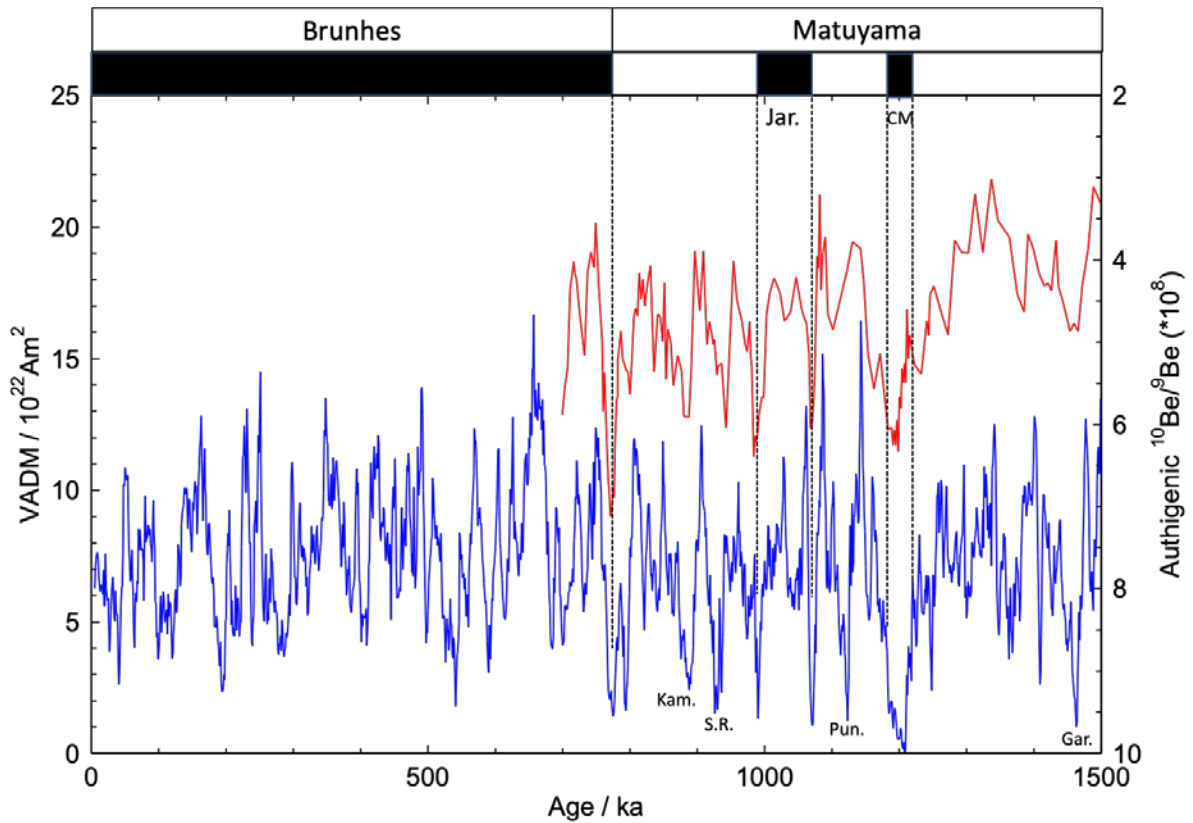
358

359 Figure 8. Palaeointensity and  $^{10}\text{Be}$  data for the last 800 kyr. Virtual axial dipole moment (VADM) from the  
 360 PISO1500 palaeointensity stack (blue) (Channell et al., 2009); VADM derived from an authigenic  $^{10}\text{Be}/^9\text{Be}$   
 361 ratio stack (Simon et al., 2016) using an empirical calibration (red); published  $^{10}\text{Be}$  fluxes from the EDC ice  
 362 core (black, right axis) (Cauquoin et al., 2015; Raisbeck et al., 2017; Raisbeck et al., 2006).

363

364 There are two aspects that degrade the ability of  $^{10}\text{Be}$  alone to provide a dating template. The first is that it is the  
 365  $^{10}\text{Be}$  flux that resembles marine data, and we will only have measurements of  $^{10}\text{Be}$  concentration. This issue  
 366 applies also to dust (as discussed above), but the dynamic range between glacial and interglacial for dust is so  
 367 great (factor 10 in marine sediments, higher still in ice) that the influence of accumulation rate changes is second  
 368 order and does not mask the signal that is common between ice and marine sediments. For  $^{10}\text{Be}$  the range of the  
 369 data (factor 2 between low and high) is similar to the range of accumulation rates, meaning that the  
 370 concentration is equally influenced by the cosmogenic production rate and the snow accumulation rate. By itself  
 371 the  $^{10}\text{Be}$  concentration will be hard to place onto the template.





372  
 373 Figure 9. Palaeointensity and authigenic  $^{10}\text{Be}/^9\text{Be}$  from marine sediments for the last 1.5 Myr. Virtual axial  
 374 dipole moment (VADM) from the PISO1500 palaeointensity stack (blue) (Channell et al., 2009); authigenic  
 375  $^{10}\text{Be}/^9\text{Be}$  (decay-corrected) from core MD97-2143 (red) (Simon et al., 2018). Each of the polarity reversals  
 376 (Brunhes, Jaramillo, Cobb Mountain) is associated with a palaeointensity low. Other prominent excursions in  
 377 the Matuyama Chron are labeled: Kam = Kamikatsura; S.R. = Santa Rosa; Pun = Punaruu; Gar = Gardar  
 378 (Channell, 2017).

379  
 380 There is one possible way to deal with this issue. The accumulation rate for the EDC core was actually a product  
 381 derived from the age modelling, but based on a prior where the accumulation rate was assumed to be directly  
 382 related to the temperature and hence to the water isotope ratios. If we assume that that relationship was  
 383 unchanged over 1.5 million years then the best fit values from the 800 kyr of EDC could be used, along with  
 384 water isotope ratios measured at LDC to estimate the accumulation rate for each depth and therefore calculate a  
 385 flux of  $^{10}\text{Be}$ . This will have considerable uncertainties but is likely to allow identification of the main features in  
 386 the expected  $^{10}\text{Be}$  record.

387 An additional problem is the one encountered when the Brunhes-Matuyama section of the EDC ice core was  
 388 analysed (Raisbeck et al., 2006), that  $^{10}\text{Be}$  in deeper ice shows spikes that appear to be inhomogeneous across  
 389 the core and may be associated with high concentrations of dust and other chemical concentrations. The spikes  
 390 have been tentatively ascribed to a concentration effect where  $^{10}\text{Be}$  becomes associated with dust particles which  
 391 also seem to clump together into aggregates in the deeper ice (de Angelis et al., 2013). For the Brunhes-  
 392 Matuyama section of the EDC ice core, the spikiness in  $^{10}\text{Be}$  was bypassed using median concentrations

393 (Raisbeck et al., 2006), and it may be that such a strategy will continue to work in older ice. However, further  
 394 work is needed to understand the conditions that lead to this effect.

395 **7. Discussion and conclusion**

396 We have presented templates for what an undisturbed (i.e., where time is monotonic with depth) ice core from  
 397 LDC might be expected to show. We summarise the 4 methods we have considered in Table 1. The marine dust  
 398 record (represented here by Fe MAR at ODP site 1090) could, with reasonable assumptions, be an excellent  
 399 template for the LDC dust record. The Mg/Ca data from site 1123, matched against the LDC water isotope  
 400 record, could provide additional validation, although the correlation between records over the past 800 kyr is  
 401 less strong than for dust. The methane data, matched against D-O variability at site U1385 may be capable of  
 402 adding some sharper tie points in a record that has already been matched to first order. <sup>10</sup>Be concentration,  
 403 converted to an estimated flux using water isotope data, should be a useful additional constraint, particularly in  
 404 identifying the major features with low Vertical Axial Dipole Moment (VADM) and expected high <sup>10</sup>Be  
 405 concentration. All of the constraints provided by this method and others would be included within a Bayesian  
 406 framework using a program such as IceChrono (Parrenin et al., 2015), which would provide an estimate of the  
 407 uncertainty.

Ice core measure	Template	Assumptions	Comments
Dust	South Atlantic marine core dust proxy	Changes in atmospheric transport do not overwhelm the common source signature	Good matches at multimillennial scale even when using ice core concentration
Water isotopes	Southern marine benthic Mg/Ca	Antarctic surface temperatures continue to drive southern deepwater temperature	Good match at orbital scale, but less good for cycles of weaker amplitude
Methane	Portuguese Margin marine planktic $\delta^{18}\text{O}$	Both records record common millennial variability	Millennial scale alignment possible, but different amplitudes for individual peaks would make it hard to use alone.
<sup>10</sup> Be	Paleointensity measures in marine cores	Both records dominated at long timescales by strength of Earth's magnetic field	Requires estimate of ice accumulation rate to derive <sup>10</sup> Be flux; statistical issues with <sup>10</sup> Be spikes need to be solved.

408

409 Table 1: Characteristics of possible template matching methods for a 1.5 million year ice core

410

411 It will be a greater challenge to use these records to aid the age modelling if the record is disturbed, with folds or  
 412 missing ice, as has often been the case with ice near the bed of ice sheets (e.g. NEEM Community Members,  
 413 2013). In that case, one cannot rely on the shape of the signal to identify the time period represented. Instead, we  
 414 are dependent on using the absolute values – for example finding a time period where the values in the templates  
 415 are all consistent with the measured values. The derived <sup>10</sup>Be production may be particularly important in this  
 416 case, because it is independent of climate and, thus, may provide a more robust age assignment compared to the  
 417 other templates considered here, which are highly correlated on glacial/interglacial time scales. This will have to  
 418 be done with considerable caution, given the uncertainties involved in the assumptions about the unchanged

419 relationship between the measured values and their marine equivalents over time. Finally an age model for the  
420 new core will of course also use other data, including those from gas measurements ( $\delta^{18}\text{O}_{\text{atm}}$  and  $\text{O}_2/\text{N}_2$ , which  
421 can be matched to calculated orbital targets), and any radiometric absolute ages that can be obtained from the  
422 limited ice volumes available.

#### 423 **Data availability**

424 All the datasets shown in this paper have already been published elsewhere, as indicated by the relevant  
425 references.

#### 426 **Author contribution**

427 All authors conceived the idea for this paper. EW prepared the first draft and all authors reviewed and edited the  
428 text.

#### 429 **Competing interests**

430 The authors declare that they have no conflict of interest.

#### 431 **Acknowledgments**

432 This publication was generated in the frame of Beyond EPICA. The project has received funding from the  
433 European Union's Horizon 2020 research and innovation programme under grant agreement No. 815384  
434 (Oldest Ice Core). It is supported by national partners and funding agencies in Belgium, Denmark, France,  
435 Germany, Italy, Norway, Sweden, Switzerland, The Netherlands and the United Kingdom. Logistic support is  
436 mainly provided by PNRA and IPEV through the Concordia Station system. The opinions expressed and  
437 arguments employed herein do not necessarily reflect the official views of the European Union funding agency  
438 or other national funding bodies. This is Beyond EPICA publication number XX. This publication is also  
439 associated with the Million Year Ice Core (MYIC) Project of the Australian Antarctic Program (AAP). We  
440 thank Alexander Cauquoin and Grant Raisbeck for advice about the published  $^{10}\text{Be}$  data. EW was supported by  
441 a Royal Society Professorship. HF acknowledges the long-term financial support of ice core science by the  
442 Swiss National Science Foundation. TvO acknowledges support by the Australian Government Department of  
443 Industry, Science, Energy and Resources (grant no. ASCI000002). We thank 4 reviewers for their helpful  
444 comments.

445

446 **References**

- 447 Ahn, S., Khider, D., Lisiecki, L. E., and Lawrence, C. E.: A probabilistic Pliocene–Pleistocene stack of  
448 benthic  $\delta^{18}\text{O}$  using a profile hidden Markov model, *Dynamics and Statistics of the Climate System*, 2,  
449 doi: 10.1093/climsys/dzx002, 2017.
- 450  
451 Baggenstos, D., Häberli, M., Schmitt, J., Shackleton, S. A., Birner, B., Severinghaus, J. P., Kellerhals, T.,  
452 and Fischer, H.: Earth’s radiative imbalance from the Last Glacial Maximum to the present,  
453 *Proceedings of the National Academy of Sciences*, 116, 14881, doi: 10.1073/pnas.1905447116, 2019.
- 454  
455 Barker, S., Knorr, G., Edwards, R. L., Parrenin, F., Putnam, A. E., Skinner, L. C., Wolff, E. W., and  
456 Ziegler, M.: 800,000 years of abrupt climate variability, *Science*, 334, 347-351, 2011.
- 457  
458 Baumgartner, M., Kindler, P., Eicher, O., Floch, G., Schilt, A., Schwander, J., Spahni, R., Capron, E.,  
459 Chappellaz, J., Leuenberger, M., Fischer, H., and Stocker, T. F.: NGRIP CH<sub>4</sub> concentration from 120 to  
460 10 kyr before present and its relation to a delta N-15 temperature reconstruction from the same ice  
461 core, *Climate of the Past*, 10, 903-920, doi: 10.5194/cp-10-903-2014, 2014.
- 462  
463 Bazin, L., Landais, A., Lemieux-Dudon, B., Kele, H. T. M., Veres, D., Parrenin, F., Martinerie, P., Ritz, C.,  
464 Capron, E., Lipenkov, V., Loutre, M. F., Raynaud, D., Vinther, B., Svensson, A., Rasmussen, S. O.,  
465 Severi, M., Blunier, T., Leuenberger, M., Fischer, H., Masson-Delmotte, V., Chappellaz, J., and Wolff,  
466 E. W.: An optimised multi-proxy, multi-site Antarctic ice and gas orbital chronology (AICC2012): 120-  
467 800 ka, *Climate of the Past* 9, 1715-1731, 2013.
- 468  
469 Bender, M. L., Barnett, B., Dreyfus, G., Jouzel, J., and Porcelli, D.: The contemporary degassing rate of  
470 <sup>40</sup>Ar from the solid Earth, *Proceedings of the National Academy of Sciences*, 105, 8232, doi:  
471 10.1073/pnas.0711679105, 2008.
- 472  
473 Bereiter, B., Eggleston, S., Schmitt, J., Nehrbass-Ahles, C., Stocker, T. F., Fischer, H., Kipfstuhl, S., and  
474 Chappellaz, J.: Revision of the EPICA Dome C CO<sub>2</sub> record from 800 to 600 kyr before present,  
475 *Geophys. Res. Lett.*, 42, 542-549, doi: 10.1002/2014GL061957, 2015.
- 476  
477 Bereiter, B., Fischer, H., Schwander, J., and Stocker, T. F.: Diffusive equilibration of N-2, O-2 and CO<sub>2</sub>  
478 mixing ratios in a 1.5-million-years-old ice core, *Cryosphere*, 8, 245-256, doi: 10.5194/tc-8-245-2014,  
479 2014.
- 480  
481 Bereiter, B., Shackleton, S., Baggenstos, D., Kawamura, K., and Severinghaus, J.: Mean global ocean  
482 temperatures during the last glacial transition, *Nature*, 553, 39, doi: 10.1038/nature25152  
483 <https://www.nature.com/articles/nature25152#supplementary-information>, 2018.
- 484  
485 Birner, B., Hodell, D. A., Tzedakis, P. C., and Skinner, L. C.: Similar millennial climate variability on the  
486 Iberian margin during two early Pleistocene glacials and MIS 3, *Paleoceanography*, 31, 203-217, doi:  
487 10.1002/2015pa002868, 2016.
- 488

489 Bock, M., Schmitt, J., Beck, J., Seth, B., Chappellaz, J., and Fischer, H.: Glacial/interglacial wetland,  
490 biomass burning, and geologic methane emissions constrained by dual stable isotopic CH<sub>4</sub> ice core  
491 records, *Proceedings of the National Academy of Sciences*, doi: 10.1073/pnas.1613883114, 2017.  
492 doi: 10.1073/pnas.1613883114, 2017.

493

494 Buizert, C., Baggenstos, D., Jiang, W., Purtschert, R., Petrenko, V. V., Lu, Z. T., Muller, P., Kuhl, T., Lee,  
495 J., Severinghaus, J. P., and Brook, E. J.: Radiometric Kr-81 dating identifies 120,000-year-old ice at  
496 Taylor Glacier, Antarctica, *Proc. Natl. Acad. Sci. U. S. A.*, 111, 6876-6881, doi:  
497 10.1073/pnas.1320329111, 2014.

498

499 Buizert, C., Fudge, T. J., Roberts, W. H. G., Steig, E. J., Sherriff-Tadano, S., Ritz, C., Lefebvre, E.,  
500 Edwards, J., Kawamura, K., Oyabu, I., Motoyama, H., Kahle, E. C., Jones, T. R., Abe-Ouchi, A., Obase,  
501 T., Martin, C., Corr, H., Severinghaus, J. P., Beaudette, R., Epifanio, J. A., Brook, E. J., Martin, K.,  
502 Chappellaz, J., Aoki, S., Nakazawa, T., Sowers, T. A., Alley, R. B., Ahn, J., Sigl, M., Severi, M., Dunbar,  
503 N. W., Svensson, A., Fegyveresi, J. M., He, C., Liu, Z., Zhu, J., Otto-Bliesner, B. L., Lipenkov, V. Y.,  
504 Kageyama, M., and Schwander, J.: Antarctic surface temperature and elevation during the Last  
505 Glacial Maximum, *Science*, 372, 1097, doi: 10.1126/science.abd2897, 2021.

506

507 Cauquoin, A.: Flux de <sup>10</sup>Be en Antarctique durant les 800 000 dernières années et interprétation.,  
508 Ph.D., Sciences de la Terre, Université Paris Sud, Paris, 205 pp., 2013.

509

510 Cauquoin, A., Landais, A., Raisbeck, G. M., Jouzel, J., Bazin, L., Kageyama, M., Peterschmitt, J. Y.,  
511 Werner, M., Bard, E., and Team, A.: Comparing past accumulation rate reconstructions in East  
512 Antarctic ice cores using <sup>10</sup>Be, water isotopes and CMIP5-PMIP3 models, *Clim. Past*, 11,  
513 355-367, doi: 10.5194/cp-11-355-2015, 2015.

514

515 Channell, J. E. T.: Magnetic excursions in the late Matuyama Chron (Olduvai to Matuyama-Brunhes  
516 boundary) from North Atlantic IODP sites, *J. Geophys. Res.-Solid Earth*, 122, 773-789, doi:  
517 10.1002/2016jb013616, 2017.

518

519 Channell, J. E. T., Xuan, C., and Hodell, D. A.: Stacking paleointensity and oxygen isotope data for the  
520 last 1.5 Myr (PISO-1500), *Earth planet. Sci. Lett.*, 283, 14-23, doi:  
521 <https://doi.org/10.1016/j.epsl.2009.03.012>, 2009.

522

523 Chappellaz, J., Stowasser, C., Blunier, T., Baslev-Clausen, D., Brook, E. J., Dallmayr, R., Fain, X., Lee, J.  
524 E., Mitchell, L. E., Pascual, O., Romanini, D., Rosen, J., and Schupbach, S.: High-resolution glacial and  
525 deglacial record of atmospheric methane by continuous-flow and laser spectrometer analysis along  
526 the NEEM ice core, *Climate of the Past*, 9, 2579-2593, doi: 10.5194/cp-9-2579-2013, 2013.

527

528 Cheng, H., Edwards, R. L., Sinha, A., Spotl, C., Yi, L., Chen, S. T., Kelly, M., Kathayat, G., Wang, X. F., Li,  
529 X. L., Kong, X. G., Wang, Y. J., Ning, Y. F., and Zhang, H. W.: The Asian monsoon over the past 640,000  
530 years and ice age terminations, *Nature*, 534, 640+, doi: 10.1038/nature18591, 2016.

531

532 Clark, P. U., Archer, D., Pollard, D., Blum, J. D., Rial, J. A., Brovkin, V., Mix, A. C., Pisias, N. G., and Roy,  
533 M.: The middle Pleistocene transition: characteristics. mechanisms, and implications for long-term

534 changes in atmospheric PCO<sub>2</sub>, *Quat. Sci. Rev.*, 25, 3150-3184, doi: 10.1016/j.quascirev.2006.07.008,  
535 2006.

536

537 Crotti, I., Landais, A., Stenni, B., Bazin, L., Parrenin, F., Frezzotti, M., Ritterbusch, F., Lu, Z.-T., Jiang,  
538 W., Yang, G.-M., Fourré, E., Orsi, A., Jacob, R., Minster, B., Prié, F., Dreossi, G., and Barbante, C.: An  
539 extension of the TALDICE ice core age scale reaching back to MIS 10.1, *Quat. Sci. Rev.*, 266, 107078,  
540 doi: <https://doi.org/10.1016/j.quascirev.2021.107078>, 2021.

541

542 de Angelis, M., Tison, J. L., Morel-Fourcade, M. C., and Susini, J.: Micro-investigation of EPICA Dome  
543 C bottom ice: evidence of long term in situ processes involving acid-salt interactions, mineral dust,  
544 and organic matter, *Quat. Sci. Rev.*, 78, 248-265, doi: 10.1016/j.quascirev.2013.08.012, 2013.

545

546 Delmas, R. J., Beer, J., Synal, H. A., Muscheler, R., Petit, J. R., and Pourchet, M.: Bomb-test Cl-36  
547 measurements in Vostok snow (Antarctica) and the use of Cl-36 as a dating tool for deep ice cores,  
548 *Tellus Ser. B-Chem. Phys. Meteorol.*, 56, 492-498, doi: 10.1111/j.1600-0889.2004.00109.x, 2004.

549

550 Delmonte, B., Andersson, P. S., Hansson, M., Schoberg, H., Petit, J. R., Basile-Doelsch, I., and Maggi,  
551 V.: Aeolian dust in East Antarctica (EPICA-Dome C and Vostok): Provenance during glacial ages over  
552 the last 800 kyr, *Geophys. Res. Lett.*, 35, L07703, doi: 10.1029/2008GL033382, 2008.

553

554 Elderfield, H., Ferretti, P., Greaves, M., Crowhurst, S., McCave, I. N., Hodell, D., and Piotrowski, A. M.:  
555 Evolution of ocean temperature and ice volume through the Mid-Pleistocene Climate Transition,  
556 *Science*, 337, 704-709, 2012.

557

558 Extier, T., Landais, A., Bréant, C., Prié, F., Bazin, L., Dreyfus, G., Roche, D. M., and Leuenberger, M.:  
559 On the use of  $\delta^{18}\text{O}_{\text{atm}}$  for ice core dating, *Quat. Sci. Rev.*, 185, 244-257, doi:  
560 <https://doi.org/10.1016/j.quascirev.2018.02.008>, 2018.

561

562 Fischer, H., Fundel, F., Ruth, U., Twarloh, B., Wegner, A., Udisti, R., Becagli, S., Castellano, E.,  
563 Morganti, A., Severi, M., Wolff, E. W., Littot, G. C., Rothlisberger, R., Mulvaney, R., Hutterli, M. A.,  
564 Kaufmann, P., Federer, U., Lambert, F., Bigler, M., Hansson, M., Jonsell, U., de Angelis, M., Gabrielli,  
565 P., Boutron, C., Siggaard-Andersen, M. L., Steffensen, J. P., Barbante, C., Gaspari, V., and Wagenbach,  
566 D.: Reconstruction of millennial changes in transport, dust emission and regional differences in sea  
567 ice coverage using the deep EPICA ice cores from the Atlantic and Indian Ocean sector of Antarctica.,  
568 *Earth planet. Sci. Lett.*, 260, 340-354, 2007a.

569

570 Fischer, H., Severinghaus, J., Brook, E., Wolff, E., Albert, M., Alemany, O., Arthern, R., Bentley, C.,  
571 Blankenship, D., Chappellaz, J., Creyts, T., Dahl-Jensen, D., Dinn, M., Frezzotti, M., Fujita, S., Galée,  
572 H., Hindmarsh, R., Hudspeth, D., Jugie, G., Kawamura, K., Lipenkov, V., Miller, H., Mulvaney, R.,  
573 Pattyn, F., Ritz, C., Schwander, J., Steinhage, D., van Ommen, T., and Wilhelms, F.: Where to find 1.5  
574 million yr old ice for the IPICS "Oldest Ice" ice core, *Climate of the Past*, 9, 2489-2505, doi:  
575 10.5194/cpd-9-2771-2013, 2013.

576

577 Fischer, H., Siggaard-Andersen, M. L., Ruth, U., Rothlisberger, R., and Wolff, E. W.: Glacial-interglacial  
578 changes in mineral dust and sea salt records in polar ice cores: sources, transport, deposition, *Rev.*  
579 *Geophys.*, 45, RG1002, doi: 10.1029/2005RG000192, 2007b.

580  
581 Ford, H. L. and Raymo, M. E.: Regional and global signals in seawater  $\delta^{18}\text{O}$  records across the mid-  
582 Pleistocene transition, *Geology*, 48, 113-117, doi: 10.1130/G46546.1, 2019.

583  
584 Giaccio, B., Regattieri, E., Zanchetta, G., Nomade, S., Renne, P. R., Sprain, C. J., Drysdale, R. N.,  
585 Tzedakis, P. C., Messina, P., Scardia, G., Sposato, A., and Bassinot, F.: Duration and dynamics of the  
586 best orbital analogue to the present interglacial, *Geology*, 43, 603-606, doi: 10.1130/G36677.1,  
587 2015.

588  
589 Govin, A., Chiessi, C. M., Zabel, M., Sawakuchi, A. O., Heslop, D., Hörner, T., Zhang, Y., and Mulitza,  
590 S.: Terrigenous input off northern South America driven by changes in Amazonian climate and the  
591 North Brazil Current retroflexion during the last 250 ka, *Clim. Past*, 10, 843-862, doi: 10.5194/cp-10-  
592 843-2014, 2014.

593  
594 Grootes, P. M., Stuiver, M., White, J. W. C., Johnsen, S., and Jouzel, J.: Comparison of oxygen isotope  
595 records from the GISP2 and GRIP Greenland ice cores, *Nature*, 366, 552-554, 1993.

596  
597 Hodell, D., Lourens, L., Crowhurst, S., Konijnendijk, T., Tjallingii, R., Jiménez-Espejo, F., Skinner, L.,  
598 Tzedakis, P. C., Abrantes, F., Acton, G. D., Alvarez Zarikian, C. A., Bahr, A., Balestra, B., Barranco, E. L.,  
599 Carrara, G., Ducassou, E., Flood, R. D., Flores, J.-A., Furota, S., Grimalt, J., Grunert, P., Hernández-  
600 Molina, J., Kim, J. K., Krissek, L. A., Kuroda, J., Li, B., Lofi, J., Margari, V., Martrat, B., Miller, M. D.,  
601 Nanayama, F., Nishida, N., Richter, C., Rodrigues, T., Rodríguez-Tovar, F. J., Roque, A. C. F., Sanchez  
602 Goñi, M. F., Sierro Sánchez, F. J., Singh, A. D., Sloss, C. R., Stow, D. A. V., Takashimizu, Y., Tzanova, A.,  
603 Voelker, A., Xuan, C., and Williams, T.: A reference time scale for Site U1385 (Shackleton Site) on the  
604 SW Iberian Margin, *Global and Planetary Change*, 133, 49-64, doi: 10.1016/j.gloplacha.2015.07.002,  
605 2015.

606  
607 Jouzel, J., Alley, R. B., Cuffey, K. M., Dansgaard, W., Grootes, P., Hoffmann, G., Johnsen, S. J., Koster,  
608 R. D., Peel, D., Shuman, C. A., Stievenard, M., Stuiver, M., and White, J.: Validity of the temperature  
609 reconstruction from water isotopes in ice cores, *J. Geophys. Res.*, 102, 26471-26487, 1997.

610  
611 Jouzel, J., Masson-Delmotte, V., Cattani, O., Dreyfus, G., Falourd, S., Hoffmann, G., Nouet, J., Barnola,  
612 J. M., Chappellaz, J., Fischer, H., Gallet, J. C., Johnsen, S., Leuenberger, M., Loulergue, L., Luethi, D.,  
613 Oerter, H., Parrenin, F., Raisbeck, G., Raynaud, D., Schwander, J., Spahni, R., Souchez, R., Selmo, E.,  
614 Schilt, A., Steffensen, J. P., Stenni, B., Stauffer, B., Stocker, T., Tison, J.-L., Werner, M., and Wolff, E.  
615 W.: Orbital and millennial Antarctic climate variability over the last 800 000 years, *Science*, 317, 793-  
616 796, doi: 10.1126/science.1141038, 2007.

617  
618 Kawamura, K., Abe-Ouchi, A., Motoyama, H., Ageta, Y., Aoki, S., Azuma, N., Fujii, Y., Fujita, K., Fujita,  
619 S., Fukui, K., Furukawa, T., Furusaki, A., Goto-Azuma, K., Greve, R., Hirabayashi, M., Hondoh, T., Hori,  
620 A., Horikawa, S., Horiuchi, K., Igarashi, M., Iizuka, Y., Kameda, T., Kanda, H., Kohno, M., Kuramoto, T.,  
621 Matsushi, Y., Miyahara, M., Miyake, T., Miyamoto, A., Nagashima, Y., Nakayama, Y., Nakazawa, T.,  
622 Nakazawa, F., Nishio, F., Obinata, I., Ohgaito, R., Oka, A., Okuno, J., Okuyama, J., Oyabu, I., Parrenin,  
623 F., Pattyn, F., Saito, F., Saito, T., Saito, T., Sakurai, T., Sasa, K., Seddik, H., Shibata, Y., Shinbori, K.,  
624 Suzuki, K., Suzuki, T., Takahashi, A., Takahashi, K., Takahashi, S., Takata, M., Tanaka, Y., Uemura, R.,  
625 Watanabe, G., Watanabe, O., Yamasaki, T., Yokoyama, K., Yoshimori, M., Yoshimoto, T., and Dome



626 Fuji Ice Core, P.: State dependence of climatic instability over the past 720,000 years from Antarctic  
627 ice cores and climate modeling, *Science Advances*, 3, doi: 10.1126/sciadv.1600446, 2017.

628  
629 Kawamura, K., Parrenin, F., Lisiecki, L., Uemura, R., Vimeux, F., Severinghaus, J. P., Hutterli, M. A.,  
630 Nakazawa, T., Aoki, S., Jouzel, J., Raymo, M. E., Matsumoto, K., Nakata, H., Motoyama, H., Fujita, S.,  
631 Azuma, K., Fujii, Y., and Watanabe, O.: Northern Hemisphere forcing of climatic cycles over the past  
632 360,000 years implied by accurately dated Antarctic ice cores, *Nature*, 448, 912-916, 2007.

633  
634 Lambert, F., Delmonte, B., Petit, J. R., Bigler, M., Kaufmann, P. R., Hutterli, M. A., Stocker, T. F., Ruth,  
635 U., Steffensen, J. P., and Maggi, V.: Dust-climate couplings over the past 800,000 years from the  
636 EPICA Dome C ice core, *Nature*, 452, 616-619, 2008.

637  
638 Lilien, D. A., Steinhage, D., Taylor, D., Parrenin, F., Ritz, C., Mulvaney, R., Martín, C., Yan, J. B., O'Neill,  
639 C., Frezzotti, M., Miller, H., Gogineni, P., Dahl-Jensen, D., and Eisen, O.: Brief communication: New  
640 radar constraints support presence of ice older than 1.5 Myr at Little Dome C, *The Cryosphere*, 15,  
641 1881-1888, doi: 10.5194/tc-15-1881-2021, 2021.

642  
643 Lisiecki, L. E. and Raymo, M. E.: Plio-Pleistocene climate evolution: trends and transitions in glacial  
644 cycle dynamics, *Quat. Sci. Rev.*, 26, 56-69, doi: 10.1016/j.quascirev.2006.09.005, 2007.

645  
646 Lisiecki, L. E. and Raymo, M. E.: A Pliocene-Pleistocene stack of 57 globally distributed benthic delta  
647 O-18 records, *Paleoceanography*, 20, PA1003, doi: 10.1029/2004PA001071, 2005.

648  
649 Louergue, L., Schilt, A., Spahni, R., Masson-Delmotte, V., Blunier, T., Lemieux, B., Barnola, J. M.,  
650 Raynaud, D., Stocker, T. F., and Chappellaz, J.: Orbital and millennial-scale features of atmospheric  
651 CH<sub>4</sub> over the last 800,000 years, *Nature*, 453, 383-386, 2008.

652  
653 Markle, B. R., Steig, E. J., Roe, G. H., Winckler, G., and McConnell, J. R.: Concomitant variability in  
654 high-latitude aerosols, water isotopes and the hydrologic cycle, *Nature Geoscience*, 11, 853-859, doi:  
655 10.1038/s41561-018-0210-9, 2018.

656  
657 Martinez-Garcia, A., Rosell-Mele, A., Jaccard, S. L., Geibert, W., Sigman, D. M., and Haug, G. H.:  
658 Southern Ocean dust-climate coupling over the past four million years, *Nature*, 476, 312-U141, doi:  
659 10.1038/nature10310, 2011.

660  
661 Muscheler, R., Adolphi, F., and Knudsen, M. F.: Assessing the differences between the IntCal and  
662 Greenland ice-core time scales for the last 14,000 years via the common cosmogenic radionuclide  
663 variations, *Quat. Sci. Rev.*, 106, 81-87, doi: 10.1016/j.quascirev.2014.08.017, 2014.

664  
665 NEEM Community Members: Eemian interglacial reconstructed from a Greenland folded ice core  
666 *Nature*, 493, 489-494, doi: 10.1038/nature11789, 2013.

667  
668 North Greenland Ice-Core Project (NorthGRIP) Members: High-resolution record of Northern  
669 Hemisphere climate extending into the last interglacial period, *Nature*, 431, 147-151, 2004.

670  
671 North Greenland Ice Core Project Members: High-resolution record of Northern Hemisphere climate  
672 extending into the last interglacial period, *Nature*, 431, 147-151, 2004.

673  
674 Parrenin, F., Bazin, L., Capron, E., Landais, A., Lemieux-Dudon, B., and Masson-Delmotte, V.:  
675 IceChrono1: a probabilistic model to compute a common and optimal chronology for several ice  
676 cores, *Geosci. Model Dev.*, 8, 1473-1492, doi: 10.5194/gmd-8-1473-2015, 2015.

677  
678 Petit, J. R. and Delmonte, B.: A model for large glacial-interglacial climate-induced changes in dust  
679 and sea salt concentrations in deep ice cores (central Antarctica): paleoclimatic implications and  
680 prospects for refining ice core chronologies, *Tellus B*, 61, 768-790, doi: 10.1111/j.1600-  
681 0889.2009.00437.x, 2009.

682  
683 Pol, K., Masson-Delmotte, V., Johnsen, S., Bigler, M., Cattani, O., Durand, G., Falourd, S., Jouzel, J.,  
684 Minster, B., Parrenin, F., Ritz, C., Steen-Larsen, H. C., and Stenni, B.: New MIS 19 EPICA Dome C high  
685 resolution deuterium data: Hints for a problematic preservation of climate variability at sub-  
686 millennial scale in the "oldest ice", *Earth planet. Sci. Lett.*, 298, 95-103, doi:  
687 10.1016/j.epsl.2010.07.030, 2010.

688  
689 Raisbeck, G. M., Cauquoin, A., Jouzel, J., Landais, A., Petit, J. R., Lipenkov, V. Y., Beer, J., Synal, H. A.,  
690 Oerter, H., Johnsen, S. J., Steffensen, J. P., Svensson, A., and Yiou, F.: An improved north-south  
691 synchronization of ice core records around the 41 kyr  $^{10}\text{Be}$  peak, *Clim. Past*, 13, 217-229, doi:  
692 10.5194/cp-13-217-2017, 2017.

693  
694 Raisbeck, G. M., Yiou, F., Cattani, O., and Jouzel, J.:  $^{10}\text{Be}$  evidence for the Matuyama-Brunhes  
695 geomagnetic reversal in the EPICA Dome C ice core, *Nature*, 444, 82-84, 2006.

696  
697 Raymo, M. E., Lisiecki, L. E., and Nisancioglu, K. H.: Plio-pleistocene ice volume, Antarctic climate,  
698 and the global delta O-18 record, *Science*, 313, 492-495, 2006.

699  
700 Rhodes, R. H., Brook, E. J., Chiang, J. C. H., Blunier, T., Maselli, O. J., McConnell, J. R., Romanini, D.,  
701 and Severinghaus, J. P.: Enhanced tropical methane production in response to iceberg discharge in  
702 the North Atlantic, *Science*, 348, 1016-1019, doi: 10.1126/science.1262005, 2015.

703  
704 Sánchez Goñi, M. F., Rodrigues, T., Hodell, D. A., Polanco-Martínez, J. M., Alonso-García, M.,  
705 Hernández-Almeida, I., Desprat, S., and Ferretti, P.: Tropically-driven climate shifts in southwestern  
706 Europe during MIS 19, a low eccentricity interglacial, *Earth planet. Sci. Lett.*, 448, 81-93, doi:  
707 <https://doi.org/10.1016/j.epsl.2016.05.018>, 2016.

708  
709 Shackleton, N. J., Hall, M. A., and Vincent, E.: Phase relationships between millennial-scale events  
710 64,000-24,000 years ago, *Paleoceanography*, 15, 565-569, 2000.

711  
712 Shackleton, S., Baggenstos, D., Menking, J. A., Dyonisius, M. N., Bereiter, B., Bauska, T. K., Rhodes, R.  
713 H., Brook, E. J., Petrenko, V. V., McConnell, J. R., Kellerhals, T., Häberli, M., Schmitt, J., Fischer, H.,  
714 and Severinghaus, J. P.: Global ocean heat content in the Last Interglacial, *Nature Geoscience*, 13,  
715 77-81, doi: 10.1038/s41561-019-0498-0, 2020.

716  
717 Shackleton, S., Menking, J. A., Brook, E., Buizert, C., Dyonisius, M. N., Petrenko, V. V., Baggenstos, D.,  
718 and Severinghaus, J. P.: Evolution of mean ocean temperature in Marine Isotope Stage 4, *Clim. Past*,  
719 17, 2273-2289, doi: 10.5194/cp-17-2273-2021, 2021.

720  
721 Shakun, J. D., Lea, D. W., Lisiecki, L. E., and Raymo, M. E.: An 800-kyr record of global surface ocean  
722 and implications for ice volume-temperature coupling, *Earth planet. Sci. Lett.*, 426, 58-68, doi:  
723 10.1016/j.epsl.2015.05.042, 2015.

724  
725 Simon, Q., Boulès, D. L., Thouveny, N., Horng, C.-S., Valet, J.-P., Bassinot, F., and Choy, S.:  
726 Cosmogenic signature of geomagnetic reversals and excursions from the Réunion event to the  
727 Matuyama–Brunhes transition (0.7–2.14 Ma interval), *Earth planet. Sci. Lett.*, 482, 510-524, doi:  
728 <https://doi.org/10.1016/j.epsl.2017.11.021>, 2018.

729  
730 Simon, Q., Thouveny, N., Boulès, D. L., Valet, J.-P., Bassinot, F., Ménabréaz, L., Guillou, V., Choy, S.,  
731 and Beaufort, L.: Authigenic  $^{10}\text{Be}/^{9}\text{Be}$  ratio signatures of the cosmogenic nuclide production linked  
732 to geomagnetic dipole moment variation since the Brunhes/Matuyama boundary, *Journal of*  
733 *Geophysical Research: Solid Earth*, 121, 7716-7741, doi: 10.1002/2016JB013335, 2016.

734  
735 Soudan, S. and Rosenthal, Y.: Deep-Sea Temperature and Ice Volume Changes Across the Pliocene-  
736 Pleistocene Climate Transitions, *Science*, 325, 306-310, doi: 10.1126/science.1169938, 2009.

737  
738 Wolff, E. W., Barbante, C., Becagli, S., Bigler, M., Boutron, C. F., Castellano, E., De Angelis, M.,  
739 Federer, U., Fischer, H., Fundel, F., Hansson, M., Hutterli, M., Jonsell, U., Karlin, T., Kaufmann, P.,  
740 Lambert, F., Littot, G. C., Mulvaney, R., Rothlisberger, R., Ruth, U., Severi, M., Siggaard-Andersen, M.  
741 L., Sime, L. C., Steffensen, J. P., Stocker, T. F., Traversi, R., Twarloh, B., Udisti, R., Wagenbach, D., and  
742 Wegner, A.: Changes in environment over the last 800,000 years from chemical analysis of the EPICA  
743 Dome C ice core, *Quat. Sci. Rev.*, 29, 285-295, doi: 10.1016/j.quascirev.2009.06.013, 2010.

744  
745 Yan, Y., Bender, M. L., Brook, E. J., Clifford, H. M., Kemeny, P. C., Kurbatov, A. V., Mackay, S.,  
746 Mayewski, P. A., Ng, J., Severinghaus, J. P., and Higgins, J. A.: Two-million-year-old snapshots of  
747 atmospheric gases from Antarctic ice, *Nature*, 574, 663-666, doi: 10.1038/s41586-019-1692-3, 2019.

748  
749